*J. Am. Chem. Soc.* **1982**, *104*, 2530–2534

# Effect of Buffer Viscosity on the Fluorescence of Bilirubin Bound to Human Serum Albumin

**Angelo A. Lamola* and Jorge Flores**

*Contribution from Bell Laboratories, Murray Hill, New Jersey 07974.*
*Received September 3, 1981*

**Abstract:** Bilirubin undergoes configurational ($E \rightarrow Z$) photoisomerization while bound to its most affinitive site on human serum albumin. The primary photochemical process leading to photoisomerization is twisting of the molecule about one of the exocyclic carbon–carbon double bonds in the excited singlet state. It is shown that the twisting process can be effectively inhibited when the bilirubin is in a rigid microenvironment. The quantum yield of fluorescence from albumin-bound bilirubin is observed to increase as the buffer viscosity is increased by addition of sucrose. In terms of the simplest scheme for relaxation of excited bilirubin, this is taken to mean that the twisting rate decreases with increasing buffer viscosity. The data, interpreted on the basis of both transition-state theory and a modified Kramer's theory, indicate that while bound to albumin bilirubin is probably not significantly exposed to the solvent milieu.

(4*Z*,15*Z*)-Bilirubin IX$\alpha$ (BR) bound in its most affinitive site on human serum albumin (HSA), undergoes several different transformations when excited with blue light.[1-7] The most

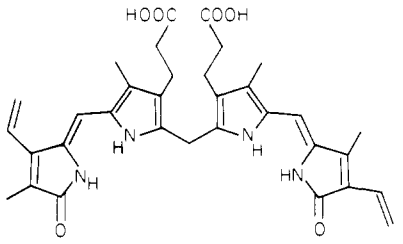


(4*Z*,15*Z*)-bilirubin IX$\alpha$

quantum efficient of these photoreactions is the reversible configurational ($Z \rightarrow E$) isomerization about one or the other exocyclic carbon–carbon double bonds.[6,8] The *E* isomers are called photobilirubin (PBR).[6] This configurational alteration is apparently the basis for the phototherapy of hyperbilirubinemia of the newborn.[4,6] Photoisomerized bilirubin appears to be excreted by the liver in the absence of glucuronyl transferase activity.[6]

The results of several different studies clearly indicate that twisting about one or the other of the exocyclic carbon–carbon double bonds in bilirubin occurs in the lowest excited singlet state. To summarize: (1) As the temperature is varied, the quantum yield of fluorescence from BR/HSA exhibits a reciprocal relation with the quantum yield of photoisomerization.[8] The fluorescence yield is about 0.002 at room temperature and 0.44 at 77 K, while the isomerization yields are 0.20 and $\leq$0.01 at these temperatures, respectively. (2) Photoexcited BR exhibits only very small (<0.01) yields of triplet states near room temperature in a variety of solvents.[9-11] Fluorescence yields under the same conditions are <0.001.[8-10] Thus, electronic relaxation of excited singlet BR near room temperature proceeds predominantly via a radiationless pathway that does not include intersystem crossing. (3) At room temperature the BR/HSA $\rightarrow$ PBR/HSA isomerization quantum yield (0.20 $\pm$ 0.02) when excited at 465 nm, an isosbestic point, is within experimental error equal to the fraction of PBR/HSA in the photoequilibrium mixture (0.22 $\pm$ 0.02).[8,12] This observation is consistent with nearly totally efficient formation of a twisted singlet state intermediate and an isomerization yield essentially equal to the fraction of twisted molecules that decay to photoisomer. (4) Difference spectra between photoexcited and nonexcited BR/HSA in aqueous buffer recorded at various times from 2 to 100 ps after excitation with 0.4-ps pulses revealed a transient assigned as the lowest excited singlet state.[8] The lifetime of the state was found to be 19 $\pm$ 3 ps at 22 °C and exhibited a temperature dependence that paralleled that of the fluorescence quantum yield. No other transient was observed. These results are consistent with a rapid decay of excited singlet molecules to a mixture of ground-state isomers via some twisted state that is even shorter lived.

BR binds to albumin at a specific high affinity ($K_a = 10^7$–$10^8$ $M^{-1}$) site.[13] It was interesting to find an isomerization rate for the protein-bound pigment of the order of 0.1 $ps^{-1}$ in light of the controversy surrounding the structural changes assigned to the ultrafast photoconversion of rhodopsin to prelumirhodsopsin (bathorhodopsin).[14] However, a more startling observation was that the decay (twisting) rate of singlet BR in chloroform solution is only marginally faster, $\tau = 15 \pm 3$ ps, than that of BR bound to HSA.[8]

The conformation of BR in any environment except for the crystal[15] is not known. It is likely, however, that BR attains substantially different conformations in chloroform solution compared with that when bound to HSA. It is suggested[16] that in solvents such as chloroform the majority species has the closed-up intramolecularly hydrogen-bonded conformation found in the crystal. The necessity to break several such hydrogen bonds

* I dedicate this paper to George S. Hammond on the occasion of his 60th birthday. The configurational photoisomerization of olefins was a central topic in Hammond's laboratory during the years I spent there as a student. It is gratifying to me to find that a similar photochemical isomerization of bilirubin forms the basis for the therapeutic effect of light upon jaundiced newborn infants. I enjoyed writing this paper especially because it relies so much upon works of Hammond and of Jack Saltiel, another Hammond student.

(1) D. A. Lightner and A. Cu, *Photochem. Photobiol.*, **26**, 427 (1977).
(2) A. F. McDonagh in "Phototherapy in the Newborn: An Overview", S. S. Gellis and A. P. Simoupolis, Eds., National Academy of Sciences, Washington, DC, 1974, pp 56–73.
(3) A. N. Cohen and J. D. Ostrow, *Pediatrics*, **65**, 740 (1980).
(4) A. A. Lamola, W. E. Blumberg, R. McClead, and A. Fanaroff, *Proc. Natl. Acad. Sci. U.S.A.*, **78**, 1882 (1981).
(5) G. Jori, E. Rossi, and F. F. Rubaltelli, *Photochem. Photobiol.*, **30**, 568 (1979).
(6) A. F. McDonagh, L. A. Palma, and D. A. Lightner, *Science (Washington, DC)* **208**, 145 (1980).
(7) D. A. Lightner, *Photochem. Photobiol.*, **26**, 427 (1977).
(8) B. I. Greene, A. A. Lamola, and C. V. Shank, *Proc. Natl. Acad. Sci. U.S.A.*, **78** 2008 (1981).
(9) E. J. Land, *Photochem. Photobiol.*, **24**, 475 (1976).
(10) R. W. Sloper and T. G. Truscott, *Photochem. Photobiol.*, **31**, 445 (1980).
(11) I. B. C. Matheson, N. U. Curry, and J. Lee, *Photochem. Photobiol.*, **31**, 115 (1980).
(12) A. A. Lamola, J. Flores, and F. H. Doleiden, *Photochem. Photobiol.*, in press.
(13) R. Brodersen, *CRC Crit. Rev. Clin. Lab. Sci.*, **11**, 305 (1979).
(14) M. Ottolenghi, *Adv. Photochem.*, **12**, 97–200 (1980).
(15) R. Bonnett, J. E. Davies, M. B. Hursthouse, and G. M. Sheldrick, *Proc. R. Soc. London, Ser. B*, **202**, 249 (1978).
(16) P. Manitto and D. Monti, *J. Chem. Soc., Chem. Commun.*, 122 (1976).

0002-7863/82/1504-2530$01.25/0 

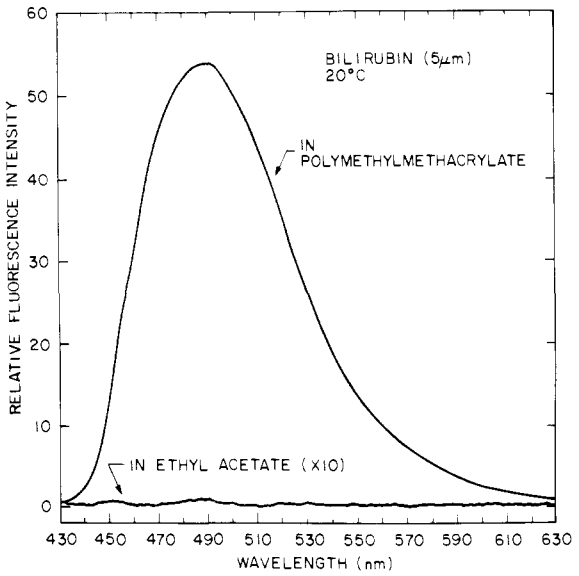


**Figure 1.** Fluorescence spectrum of bilirubin dissolved in solid polymethylmethacrylate at 20 °C ($\lambda_{ex}$ 430 nm). The signal recorded under identical conditions of measurement from a sample of bilirubin at the same concentration in ethyl acetate is shown for comparison.

may provide the major barrier to twisting of excited BR in chloroform. Such a barrier could slow the twisting rate to be comparable to that for BR bound to HSA for which it is expected that many of the hydrophilic centers of the pigment form hydrogen bonds or salt bridges with peptide residues. However, it appears remarkable that the protein causes no significant additional slowing of the isomerization rate due to steric hindrance.

One model for binding of BR to HSA that accommodates the apparent relative freedom toward photoisomerization suggests that the part of the pigment in which twisting occurs is not intimately associated with the protein. That is, BR is bound in such a way that at least one terminal pyrrole ring is free to rotate upon photoexcitation of the pigment. In bringing together the results of a variety of biochemical studies of albumin and its interactions with bilirubin, Brodersen has, in fact, suggested such a structure for BR/HSA.[13] In this model the high affinity site for BR is a trough formed by three helical sections of the protein. One dipyrrole grouping of the pigment resides in the trough and the other remains outside, exposed to the aqueous milieu.

We have found that the association constant for PBR/HSA is only about 2-fold smaller than that for BR/HSA.[17] This observation is consistent with the Brodersen model which would predict that pigment binding might not be very sensitive to the configuration of the outside dipyrrole moiety.

If the isomerizable portion of BR/HSA is indeed exposed to the aqueous milieu, we reasoned that the twisting rate might be sensitive to the solvent viscosity in analogy to the viscosity dependence of other rapid isomerization processes such as the direct photoisomerization of stilbene.[18] Therefore we measured the BR/HSA fluorescence yield, which is directly related to the twisting rate in the excited state, as a function of the concentration of sucrose added to the buffer.

## Results and Discussion

**Fluorescence of Bilirubin in Poly(methyl methacrylate).** High fluorescence yields (>0.1) from bilirubin have previously been reported for solutions frozen at very low temperatures.[1] Whether the reduction in nonradiative relaxation rates observed at the low temperatures compared with room temperature was due primarily to the rigidity of the matrices or to an intrinsic thermal barrier to radiationless relaxation in bilirubin could not be ascertained. Preliminary to the present study of the effect of buffer viscosity upon the fluorescence of albumin-bound bilirubin, it was decided to test the effect of matrix rigidity upon bilirubin fluoresence at room temperature.

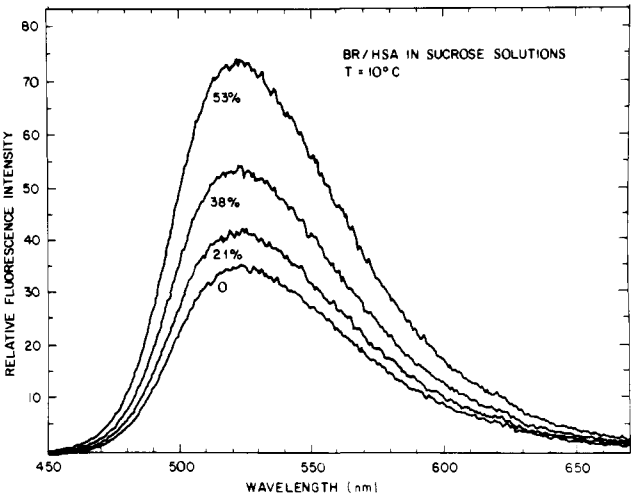


**Figure 2.** Fluorescence spectra recorded from solutions of albumin-bound bilirubin ($\lambda_{ex}$ 465 nm) containing various amounts of sucrose in the buffer.

Table I. Fluorescence Yields for BR/HSA at Various Temperatures in Buffers Containing Various Sucrose Concentrations

| % sucrose (w/w) | $10^3\phi_f$ at $T$, °C | | | | | |
|---|---|---|---|---|---|---|
| | 20 | 15 | 10 | 5 | 0 | −5 |
| 0 | 2.0 | 2.5 | 2.9 | 3.3 | 4.1 | 5.1 |
| 21 | 2.2 | 2.6 | 3.1 | 3.6 | 4.5 | |
| 38 | 2.6 | 3.2 | 3.7 | 4.3 | 5.3 | |
| 53 | 3.3 | 4.0 | 4.4 | 5.6 | 6.8 | |

The fluorescence yield of BR poly(methyl methacrylate) (spectrum shown in Figure 1) was found to be 0.33 ± 0.04 over the temperature range from 0 to 22 °C. This value is about 0.75 that of the yield observed for BR/HSA at 77 K. Whether the fluorescence yield of BR in the polymer is even higher at very low temperatures was not investigated. In contrast to the high values in poly(methyl methacrylate), bona fide fluorescence of BR in ethyl acetate at 22 °C was not observed and a confident upper limit of 0.0005 can be placed on the yield (see Figure 1). The fluorescence of BR in the polymer was observed to be unchanged after irradiation (430 nm) with a fluence three times that sufficient to cause a 22% decrease of fluorescence intensity from BR/HSA due to formation of a photostationary mixture of BR and PBR. Thus, is appears that the rigid amorphous matrix of poly(methyl methacrylate) effectively inhibits photoisomerization of bilirubin at room temperature.

**Fluorescence of BR/HSA in Sucrose/Saline Solutions.** Corrected fluorescence spectra were recorded from solutions of BR (10 μM), excess HSA (200 μM), and various amounts of sucrose in phosphate-buffered saline (pH 7.4) at various temperatures between 0 and 20 °C. Some spectra are shown in Figure 2. While all the spectra were identical in shape and position within the accuracy of the measurement, the intensity increased with increasing sucrose concentration at every temperature examined.

Independent of whatever other effects the addition of sucrose may have had, the fluorescence intensity was expected to increase by virtue of the increase in refractive index ($n$) of the buffer. The radiative transition rate increases as $n^2$.[19] All else being equal, the fluorescence yield should have increased as $n^2$. Because the samples were optically thin, the absorbance due to bilirubin should also have increased as $n^2$. Therefore, the observed fluorescence intensities were corrected for the changes in refractive index by

(17) A. A. Lamola and J. Flores, submitted for publication in *Biochem. Biophys. Res. Commun.*

(18) J. Saltiel and J. T. D'Agostino, *J. Am. Chem. Soc.*, **94**, 6445 (1972).

(19) P. Pringsheim, "Fluorescence and Phosphorescence", Interscience, New York, 1949.

Table II. Activation Parameters

Plots of log $k_t$ vs. $10^3/T$[a]

| % sucrose | slope | intercept | $E_a$, kJ/mol | $10^{14}A$ | $E_\eta$, kJ/mol[b] |
|---|---|---|---|---|---|
| 0 | −1.21 | 14.85 | 23 | 7.1 | 19 |
| 21 | −1.21 | 14.79 | 23 | 6.2 | 22 |
| 38 | −1.17 | 14.58 | 22 | 3.8 | 28 |
| 53 | −1.20 | 14.54 | 23 | 3.6 | 39 |

Plots of log $(\phi^{-1} - 2)$ vs. log $\eta$[c]

| constant % sucrose | | | constant $T$ | |
|---|---|---|---|---|
| % sucrose | slope | $E_a$, kJ/mol | $T$, °C | slope |
| 0 | −1.20 | 23 | 20 | −0.162 |
| 21 | −1.04 | 23 | 15 | −0.120 |
| 38 | −0.78 | 22 | 10 | −0.152 |
| 53 | −0.53 | 21 | 5 | −0.147 |
| | | | 0 | −0.130 |
| | | | av | −0.142 ± 0.014 |

[a] See Figure 3. [b] From plots of log $\eta$ vs. $1/T$. [c] See Figure 4.

$(n_0/n)^4$, where $n_0$ is the index of refraction of water at 20 °C and $n$ is the index of refraction of the buffer at the temperature used. Fluorescence yields calculated from the fluorescence intensities normalized in this way are listed in Table I.

**Fluorescence Yield and Rate of Primary Process.** All the observations mentioned earlier are consistent with the mechanism shown in Scheme I for the configurational isomerization of BR

**Scheme I**

$$BR \xrightarrow{h\nu} {}^1BR \quad (1)$$

$${}^1BR \xrightarrow{k_f} BR \quad (2)$$

$${}^1BR \xrightarrow{k_{is}} {}^3BR \quad (3)$$

$${}^1BR \xrightarrow{k_{ic}} BR \quad (4)$$

$${}^1BR \xrightarrow{k_t} {}^1tBR \quad (5)$$

$${}^1tBR \xrightarrow{k_d} \alpha BR + (1 - \alpha)PBR \quad (6)$$

bound to HSA. In eq 1–6 the superscripts 1 and 3 represent excited singlet and triplet states, respectively; $k_f$, $k_{is}$, $k_{ic}$, $k_t$, and $k_d$ are the rate constants for fluorescence, intersystem crossing, internal conversion to ground state without twisting, twisting of excited singlet BR, and decay of the twisted intermediate ($^1$tBR), respectively; and $\alpha$ and $(1 - \alpha)$ are the fractions of $^1$tBR that decay to BR and PBR, respectively.

The fluorescence quantum yield ($\Phi_f$) of BR/HSA is, according to this mechanism

$$\Phi_f = k_f(k_f + k_{is} + k_{ic} + k_t)^{-1} \quad (7)$$

from which the rate of twisting in the excited state may be obtained:

$$k_t = k_f[\Phi_f^{-1} - (k_{is} + k_{ic})k_f^{-1} - 1] \quad (8)$$

The limiting (low-temperature fluorescence yield of BR/HSA under conditions where little or no isomerization takes place is about 0.5.[8] Assuming $k_{is}$, $k_{ic}$, and $k_f$ are temperature independent gives $(k_{is} + k_{ic})k_f^{-1} = 1$. The value for $k_f$ (measured at 77 K) is $1.1 \times 10^8$ s$^{-1}$.[8] Thus

$$k_t = (1.1 \times 10^8)(\Phi_f^{-1} - 2) \quad (9)$$

The temperature dependence of $k_t$ may be described by the Arrhenius relation

$$k_t = Ae^{-E_a/RT} \quad (10)$$

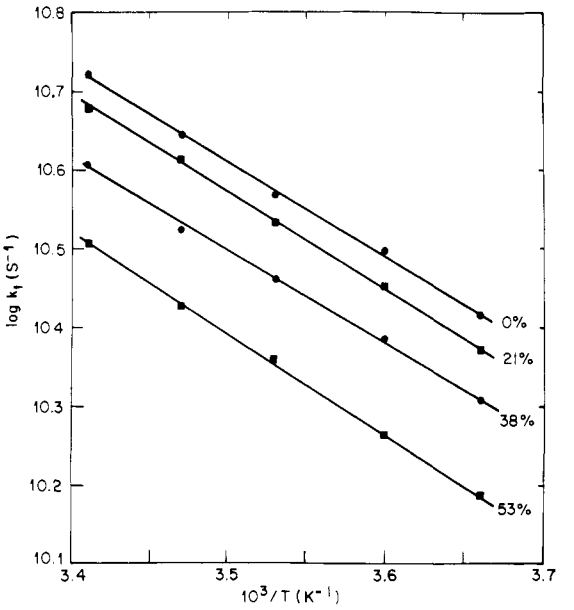


**Figure 3.** Plots of log $k_t$ vs. $10^3/T$ for solutions of alubumin-bound bilirubin containing various amounts of sucrose in the buffer. Values of $k_t$ were calculated from the data of Table I by using eq 9. The lines through the data points are the best (least-squares) linear fits.

where $A$ and $E_a$ have the usual meanings. A plot of log $[k_f(\Phi_f^{-1} - 2)]$ vs. $T^{-1}$ is given in Figure 3. It can be seen that an excellent linear fit (least squares) of the data at each sucrose concentration is obtained. Values of $E_a$ and $A$ obtained from the fitted lines are listed in Table II. While the preexponential factor, $A$, decreases with increasing sucrose concentration, the activation energy, $E_a$, was unchanged within experimental error.

Beece et al. made similar observations on the effect of increasing glycerol concentration on the rates of the various steps in the bacteriorhodopsin photocycle, namely, preexponential factors decreased with increased glycerol concentration, but activation energies were unchanged.[20] In contrast Saltiel and D'Agostino[18] observed a substantial increase in both the activation energy and preexponential factor for twisting in the excited singlet state of *trans*-stilbene on going from methylcyclohexane to glycerol as solvent.

**Assessment of the Solvent Viscosity Dependent Barrier.** Following Saltiel and D'Agostino[18] the overall activation energy $E_a$ is expressed as the sum of a solvent viscosity dependent barrier ($E_v$) and a barrier that is solvent viscosity independent ($E_i$)

$$E_a = E_v + E_i \quad (11)$$

The barriers $E_v$ and $E_i$ are associated with solvent viscosity dependent and solvent viscosity independent "rate constants", $k_v$ and $k_i$, respectively. That is to say

$$\ln k_t = \ln k_v + \ln k_i \quad (12)$$

The temperature dependence of liquid viscosity is given by the Carrancio–Andrade expression[21]

$$\ln \eta = \eta_0 + E_\eta/RT \quad (13)$$

where $\eta$ is the viscosity and $E_\eta$ is the barrier for viscous flow. Plots (not shown) of ln $\eta$ vs. $T^{-1}$ for the five buffers used gave excellent linear fits. The $E_\eta$ values obtained from the slopes of the plots are listed in Table II. Equation 12 can be expressed in Arrhenius form as

$$\ln k_t = \ln A_v + \ln A_i - (E_v + E_i)/RT \quad (14)$$

(20) D. Beece, S. F. Bowne, J. Czege, et al., submitted for publication in *Photochem. Photobiol.*

(21) W. J. Moore, "Physical Chemistry", Prentice-Hall, Englewood Cliffs, NJ, 1962, p 723.

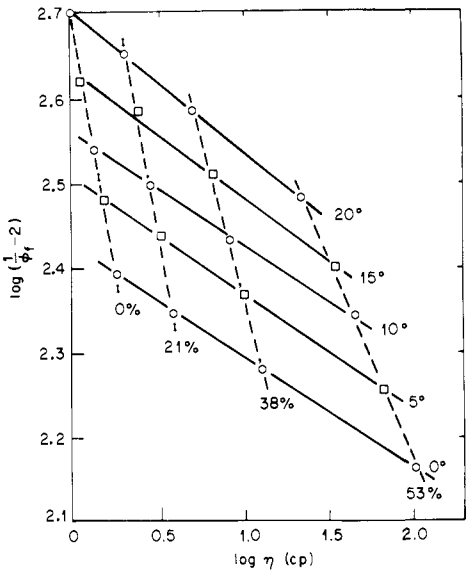


**Figure 4.** Values of log ($\Phi_f^{-1}$ − 2) obtained at various temperatures and buffer sucrose concentrations plotted against log $\eta$ where $\eta$ is the buffer viscosity. Solid lines (best linear fits by least squares) connect constant temperature points and dashed lines (best linear fits by least squares) connect points of constant sucrose concentration.

To relate temperature and viscosity changes, eq 14 is combined with eq 13:

$$\ln k_i = \ln A_v + \ln A_i + [(E_v + E_i)/E_\eta] \ln \eta_0 - [(E_v + E_i)/E_\eta] \ln \eta \quad (15)$$

Figure 4 shows plots of log ($\Phi_f^{-1}$ − 2), that is log $k_i/(1.1 \times 10^8)$, vs. log $\eta$. The dashed lines are least-squares linear fits to data points obtained at the same sucrose concentration but at different temperatures. Equation 15 predicts such linear fits to the extent that ln $\eta$ varies linearly with $1/T$ over the temperature range. Values of $E_a$, that is, $(E_v + E_i)$, can be obtained from the slopes of the dashed lines of Figure 4 and the values for $E_\eta$. Values for $E_a$ obtained in this way are listed in Table II. The good agreement among $E_a$ values obtained in the two ways simply reflects an internal consistency of the data and gives no information about the solvent viscosity dependent barrier.

To isolate the solvent viscosity barrier, eq 15 may be rewritten as

$$\ln k_i = \ln A_i + \ln A_v - (E_i/RT) + (E_v/E_\eta) \ln \eta_0 - (E_v/E_\eta) \ln \eta \quad (16)$$

The solid lines in Figure 4 connect data points obtained at the same temperature in buffers containing different sucrose concentrations. According to eq 16 the slopes of the constant temperature lines give $-(E_v/E_\eta)$. The values for the slopes are listed in Table II. The average value is 0.14 ± 0.02. The average value of $E_v$ is calculated to be 3.8 kJ/mol or about 17% of $E_a$.

The solvent viscosity independent barrier, according to the model of eq 16, should be given by the slope of the plot of log ($\Phi_f^{-1}$ − 2) vs. $1/T$ at constant viscosity. Measurements were not made in this way. However, values of ($\Phi_f^{-1}$ − 2) at constant $\eta$ for different values of $T$ can be obtained from Figure 4 by reading the intersection points of a vertical line at some value of $\eta$ with the fitted solid lines. From a plot (not shown) of log ($\Phi_f^{-1}$ − 2) vs. $1/T$ for $\eta$ = 10 cp, the value 19 ± 2 kj/mol was obtained for $E_i$, again attesting to the internal consistency of the data.

**An Alternative Model.** Beece et al. have recently examined the solvent viscosity dependence of the kinetics of the reversible photodissociations of oxymyoglobin and carbonylmyoglobin and the kinetics of the photocycle of bacteriorhodopsin.[20,22] They found that they could not satisfactorily interpret the observations on the basis of standard transition-state theory and went on to apply an approach introduced by Kramers.[23] Unlike transition-state theory, the Kramers theory introduces the viscosity of the medium into the description of molecular rate processes in an explicit manner. In the theory, escape from a potential well is critically dependent on the strength of coupling to the medium. The coupling strength is taken to be proportional to the viscosity. In addition, Beece et al.[22] point out that the barriers experienced by a ligand that is moving or undergoing geometric alteration while bound to a protein are neither static nor temperature independent because of rapid dynamic fluctuations ("breathing") of the protein itself. They further point out that such a dynamic system should be influenced by damping (viscosity of the solvent). Consequently separation of protein from solvent influences on ligand kinetics, and, therefore, separation of temperature and viscosity effects upon ligand kinetics, is complicated.

To fit their data, Beece et al. introduced a modified form of Kramers equation:

$$k(T,\eta) = [A\eta^{-\kappa} + A^0]e^{-H/RT} \quad (17)$$

where $k$ is the temperature and viscosity dependent rate constant for some ligand process and $H$ is the activation enthalpy. The parameter $A^0$ was added to supply one viscosity independent term to account for the possibility that in the very high solvent viscosity limit residual internal motion of the protein may still occur. The $A$ coefficients may also contain entropy terms.

The attenuation factor, $\kappa$, is of particular interest here. Beece et al.[20,22] reasoned that the damping of motions of residues that "stick out" into the solvent will be largely determined by the solvent viscosity ($\kappa$ = 1), while the solvent viscosity dependent damping of motion in a region inside the protein may be attenuated ($\kappa$ < 1). According to eq 17 the slopes of the constant temperature lines of Figure 4 should be equal to $-\kappa$. Thus the value of $\kappa$ obtained is 0.14 ± 0.02.

**The Albumin Binding Site for Bilirubin.** Within the context of the transition-state theoretical approach, the data indicate that of the 23 kJ/mol barrier associated with torsional motion about an exocyclic double bond of bilirubin bound to human serum albumin in water/sucrose mixtures ($E_\eta \approx$ 25 kJ/mol), about 4 kJ/mol is related to activated motions of molecules comprising the solvent. What can be concluded about the albumin binding site for bilirubin based upon these barrier values?

It is instructive to compare the observations on the BR/HSA system with those for stilbene in solution. Saltiel and D'Agostino[18] found that of the 41 kJ/mol barrier for twisting of the excited singlet state of stilbene in glycerol ($E_\eta$ = 63 kJ/mol), 26 kJ/mol could be ascribed to the solvent viscosity. In methylcyclohexane ($E_\eta$ = 10 kJ/mol), a fluid of low viscosity, 2 kJ/mol of a total barrier of 8 kJ/mol could be ascribed to a solvent viscosity barrier. Thus, it may be concluded that the solvent viscosity dependent barrier observed for BR/HSA in water/sucrose mixtures is significant but appears to play a modest role in controlling torsional twisting. Furthermore, a portion of the solvent viscosity dependent barrier may be exerted indirectly by its influence on local motions of the albumin. Thus the barrier to rotation presented by solvent molecules in direct contact with bilirubin moieties may be smaller than 4 kJ/mol. It appears, then, that a model for binding of bilirubin to albumin in which a significant portion of the bilirubin molecule is exposed to solvent molecules is not supported by the observations.

The solvent viscosity independent barrier must in part be due to constraints to twisting imposed by the protein as well as to constraints imposed by intramolecular hydrogen bonding. It is interesting that the magnitude of this barrier, 19 kJ/mol, is also modest, corresponding to the energy of between one and two hydrogen bonds.

It should be pointed out that it may not be appropriate to apply transition-state theory to the exceedingly fast (~10-ps) torsional twisting in excited bilirubin. It is interesting that the modified

(22) D. Beece, L. Eisenstein, H. Frauenfelder, et al., *Biochemistry*, **19**, 5147 (1980).

(23) H. A. Kramers, *Physica (Amsterdam)*, **7**, 284 (1940).

Kramer's theory of Beece et al., which provides explicitly for nonstatic barriers and for coupling to the solvent motion, leads to a similar conclusion for the BR/HSA system. The observed value of $\kappa$, 0.14, according to Beece et al., is consistent with the bilirubin being bound in a relatively rigid protein pocket with at least that portion of the molecule that twists probably not exposed to the aqueous medium. Within the protein pocket, bilirubin must be relatively free to isomerize.

### Experimental Section

**Materials.** (*Z*,*Z*)-Bilirubin IX$\alpha$, obtained from Sigma Chem. Co., was purified by washing a chloroform solution of it with aqueous $NaHCO_3$ according to Lightner, et al.[24] Defatted human serum albumin was prepared from fresh blood according to methods described previously.[25] Sucrose, density gradient grade, was also purchased from Sigma Chem. Co.

Bilirubin in solid poly(methyl methacrylate) was prepared as follows. Bilirubin (4.5 $\mu$M) was dissolved in freshly distilled methyl methacrylate and the solution placed in a 12-mm diameter Pyrex tube equipped for sealing. After degassing by the freeze-pump-thaw method, the tube was sealed and placed in an oven at 60 °C. The clear solid polymer obtained after 4 days was removed from the tube was machined to a 1 × 0.3 × 0.3 cm block, and the faces of the block were polished. The absorption spectrum of bilirubin in the polymer was virtually identical with that in the monomer solution. The concentration of bilirubin in the polymer block was close to 5 $\mu$M due to the contraction upon polymerization.

**Quantum Yield Measurements.** Quantitative spectrofluorometry was performed using a computer-controlled photon-counting spectrofluorometer. This instrument is equipped to correct for excitation light intensity variation and for the wavelength dependence of detection sensitivity. The optical configuration was such that intensity measurements were independent of the index of refraction of the sample (for constant sample absorbance and fluorescence yield). The variation in repeated intensity measurements was less than 5%.

Quantum yield values were determined by comparing integrated fluorescence intensities against those obtained from solutions of acridine yellow in ethanol (matched for absorbance at the excitation wavelength) for which a fluorescence yield value of 0.86 was previously determined.[26]

**Values of Viscosity and Refractive Index.** Viscosity and refractive index values for water and aqueous sucrose solutions were obtained from various published tables.[27,28] Plots of values from these tables were made when it was necessary to interpolate between table entries.

**Acknowledgment.** We thank William E. Blumberg for helpful discussions and F. H. Doleiden for technical assistance.

(24) D. A. Lightner, T. A. Wooldridge, and A. F. McDonagh, *Proc. Natl. Acad. Sci. U.S.A.*, **76**, 29 (1979).
(25) A. A. Lamola, J. Eisinger, W. E. Blumberg, et al., *Anal. Biochem.*, **100**, 25 (1979).
(26) I. B. Berlman, "Handbook of Fluorescence Spectra of Aromatic Molecules", Academic Press, New York, 1971, p 407.
(27) "National Research Council International Critical Tables of Numerical Data, Physics, Chemistry, and Technology", Vol. II, McGraw-Hill, New York, 1927, pp 337-344.
(28) "Handbook of Chemistry and Physics", 53rd ed., CRC Press, Cleveland, OH, 1972, p E211, D218.

# Platinum Metal Surface Chemistry of Benzene and Toluene

**Min-Chi Tsai and E. L. Muetterties***

*Contribution from the Materials and Molecular Research Division, Lawrence Berkeley Laboratory, and Department of Chemistry, University of California, Berkeley, California 94720.*
*Received September 3, 1981*

**Abstract:** The coordination chemistry of benzene and toluene on Pt(111) and Pt[6(111)×(111)] has been defined by thermal desorption spectrometry, isotopic labeling studies, and chemical displacement reactions. Benzene chemisorption was largely molecular (nondissociative) on Pt(111) but less so on the stepped surface. At temperatures above 100 °C, reversible benzene desorption and benzene decomposition were competing reactions. More than one *differentiable* benzene chemisorption state was present on both surfaces. Exchange experiments established that the rate of surface migration of chemisorbed benzene *between* states on these surfaces was very low. One sharp distinction in the benzene chemistry of the two platinum surfaces was that *reversible* C–H bond breaking occurred on the stepped surface but not on Pt(111). Whereas toluene chemisorption on nickel surfaces is fully irreversible, toluene chemisorbed on Pt(111) was partially desorbed as the toluene molecule at 70–110 °C. Studies with $C_6H_5CD_3$ and $C_6D_5CH_3$ suggested that the faster low-temperature C–H bond breaking process is centered on the methyl-group C–H bonds. Chemisorption of mesitylene and *m*-xylene on Pt(111) was partially reversible.

### Introduction

Earlier studies established the coordination chemistry of benzene and toluene on the low Miller index planes of nickel and on a stepped and a stepped-kinked nickel surface.[1] This coordination chemistry study was effected under ultra-high-vacuum conditions; the primary diagnostic or characterization techniques were Auger electron spectroscopy, low-energy electron diffraction, thermal desorption spectrometry, isotopic labeling studies, and chemical displacement reactions.[2,3] We describe here an analogous study of benzene and toluene chemisorption on an atomically flat and a stepped platinum surface, Pt(111) and Pt[6(111)×(111)]. Distinctive and important differences in this arene chemistry between platinum and nickel surfaces were established.

Address correspondence to this author at the Department of Chemistry, University of California.

### Experimental Section

**Reagents and Procedures.** Toluene (reagent grade), toluene-$d_8$ (Aldrich Chemical Co., 99+%), benzene (reagent grade), and benzene-$d_6$ (Aldrich Chemical Co., 99+%) were dried over calcium hydride prior to use. $C_6D_5CH_3$ and $C_6H_5CD_3$ obtained from Merck and Co. were used without treatment (traces of moisture did not detectably affect the surface chemistry). Hydrogen (Matheson, 99.95%) and deuterium (Liquid Carbonic, 99.7%) were used without further purification. Trimethylphosphine was prepared and purified as described earlier.[1]

(1) (a) Friend, C. M.; Muetterties, E. L. *J. Am. Chem. Soc.* **1981**, *103*, 773. (b) These were the nickel (111), (110), (100), 9(111)×(111), and 7(111)×(310) surfaces.
(2) Friend, C. M.; Gavin, R. M.; Muetterties, E. L.; Tsai, M.-C. *J. Am. Chem. Soc.* **1980**, *102*, 1717.
(3) Muetterties, E. L.; Tsai, M.-C. *Bull. Soc. Chim. Belg.* **1980**, *89*, 813.

0002-7863/82/1504-2534$01.25/0 